ARMY RESEARCH LABORATORY

Critical Assessment of Selected Urban Microclimate Model Frameworks

by Arnold Tunick

ARL-MR-619 **June 2005**

NOTICES

Disclaimers

The findings in this report are not to be construed as an official Department of the Army position unless so designated by other authorized documents.

Citation of manufacturer's or trade names does not constitute an official endorsement or approval of the use thereof.

Destroy this report when it is no longer needed. Do not return it to the originator.

Army Research Laboratory
Adelphi, MD 20783-1197

ARL-MR-619 **June 2005**

Critical Assessment of Selected Urban Microclimate Model Frameworks

Arnold Tunick
Computational and Information Sciences Directorate, ARL

REPORT DOCUMENTATION PAGE

Form Approved
OMB No. 0704-0188

1. REPORT DATE *(DD-MM-YYYY)*	2. REPORT TYPE	3. DATES COVERED (From - To)
June 2005	Final	October 2004 to April 2005

4. TITLE AND SUBTITLE
Critical Assessment of Selected Urban Microclimate Model Frameworks

5a. CONTRACT NUMBER

5b. GRANT NUMBER

5c. PROGRAM ELEMENT NUMBER

6. AUTHOR(S)
Arnold Tunick

5d. PROJECT NUMBER

5e. TASK NUMBER

5f. WORK UNIT NUMBER

7. PERFORMING ORGANIZATION NAME(S) AND ADDRESS(ES)
U.S. Army Research Laboratory
ATTN: AMSRD-ARL-CI-CN
2800 Powder Mill Road
Adelphi, MD 20783-1197

8. PERFORMING ORGANIZATION REPORT NUMBER
ARL-MR-619

9. SPONSORING/MONITORING AGENCY NAME(S) AND ADDRESS(ES)
U.S. Army Research Laboratory
2800 Powder Mill Road
Adelphi, MD 20783-1197

10. SPONSOR/MONITOR'S ACRONYM(S)

11. SPONSOR/MONITOR'S REPORT NUMBER(S)

12. DISTRIBUTION/AVAILABILITY STATEMENT
.Approved for public release; distribution unlimited.

13. SUPPLEMENTARY NOTES

14. ABSTRACT

This paper presents a critical assessment of six computational fluid dynamics (CFD) models. This study describes a few complex CFD frameworks in order to better understand the considerable task that is undertaken when attempting to develop such software. The paper focuses on models that were developed to simulate wind flow and the thermal microclimate around single and/or multiple buildings. Two of the selected models account for one or more embedded tree arrays. Additional information is provided regarding numerical methods, physics/turbulence algorithms, model domain, grid spacing, time-step, runtime, and computer platform. The main difficulties and/or deficiencies with each modeling approach are also discussed. It is anticipated that this study (overall) will provide much useful information, from which to initiate new modeling efforts.

15. SUBJECT TERMS
computational fluid dynamics; wind flow; buildings; conservation equations

16. SECURITY CLASSIFICATION OF:			17. LIMITATION OF ABSTRACT	18. NUMBER OF PAGES	19a. NAME OF RESPONSIBLE PERSON
a. REPORT	b. ABSTRACT	c. THIS PAGE			Arnold Tunick
Unclassified	Unclassified	Unclassified	SAR	36	19b. TELEPHONE NUMBER (*Include area code*) (301) 394-1765

Standard Form 298 (Rev. 8/98)
Prescribed by ANSI Std. Z39.18

Contents

List of Figures iv

List of Tables iv

Acknowledgment v

1. Introduction 1

2. Model Survey 2

2.1 Three-Dimensional (3-D) Finite Difference Model (Multiple buildings with an embedded array of trees) 4

2.2 Three-Dimensional (3-D) Finite Difference Model – RANS (Pedestrian winds around tall buildings) 8

2.3 Three-Dimensional (3-D) Finite Control Volume Model (Single building and/or urban street canyon) 10

2.4 Three Dimensional (3-D) Finite Volume – RANS (Multiple building array) 14

2.5 Three Dimensional (3-D) Finite Volume – LES (Multiple buildings; Central business district) 16

2.6 Three Dimensional (3-D) Finite Element – RANS (Single complex building surrounded by a complex array of trees) 17

3. Discussion 20

3.1 Finite Difference Method 20

3.2 Finite Volume Method 21

3.3 Finite Element Method 22

4. Summary and Conclusions 23

Literature Cited 24

Distribution List 27

List of Figures

Figure 1. Schematic of the building geometry for an ENVI-met model case study. Outer buildings are 24 m in height and center buildings are 15 m. Some trees are planted along the upper street canyon (from Bruse and Fleer [*3*]). 6

Figure 2. An ENVI-met model calculation of the horizontal wind field at z = 2 m, where the initial wind direction is $\theta = 90°$ (from Bruse and Fleer [*3*]). 7

Figure 3. An ENVI-met model calculation of the (normalized) temperature field at z = 2 m. The grey area indicates a central park with trees. Different surface temperatures result due to shading by buildings and trees. These effects produce a pattern of warmer (w) or colder (c) areas than the average reference temperature at the same level (from Bruse and Fleer [*3*]). 8

Figure 4. A PUMA model calculation of the horizontal wind field at z =2m, i.e., wind velocity contours (a) and wind velocity vectors (b) (from Wang et al. [*6*]). 10

Figure 5. Example wind velocity vectors computed from the CITY model (from Paterson and Apelt [*10*]). 12

Figure 6. A schematic (geometry) for the coupled wind flow and urban thermal microclimate model described in Herbert et al., (*13*). 13

Figure 7. Example results from the coupled wind flow and thermal microclimate model, i.e., predicted air temperatures (°C) across an urban canyon at 1 p.m. on 15 March (from Herbert and Herbert [*14*]).....14

Figure 8. The wind vector fields from the CFD model of Kim and Baik (*15*) at (a) z/H = 0.5 and (b) y/H = -0.75 for the case where the initial wind direction is $\theta = 45°$. 16

Figure 9. A contour plot of wind velocities for air flowing across the Washington, DC mall (from Boris [*22*]). 17

Figure 10. A schematic of the building geometry for the case study described by Calhoun et al., (*25*). The circular and the rectangular shaded regions are tree locations surrounding the building. 19

Figure 11. Example results (modeled wind vectors versus experimental data) from the FEM3 code. White vectors are experimental data and black vectors are model data. Background shading represents modeled momentum, where low momentum is dark and high momentum is lighter (from Calhoun et al., [*25*]). 20

List of Tables

Table1. Comparison of CFD models. 3

Acknowledgment

The author gratefully acknowledges Ronald Meyers and Keith Deacon of the U.S. Army Research Laboratory for offering helpful comments and discussions on this topic.

INTENTIONALLY LEFT BLANK.

1. Introduction

Rapid characterization of complex urban environments via physics-based numerical modeling will likely provide important information to U.S. Army Soldiers on the performance of advanced sensors, as well as the effectiveness of computer aids to increase situational awareness. However, two current (and extensive) surveys of the literature (*1*,*2*) indicate that computer simulation of wind flow and temperatures around complex urban structures have most often been achieved via intricate computational fluid dynamics (CFD) codes, which are (as a rule) quite computationally intensive. For example, CFD codes can require 1 to 8 hours of execution time on multiprocessor super-computers. In addition, many of the CFD models described in current literature have been in use and/or in development for 10 or more years. Also, CFD models are generally cumbersome to modify and debug. Hence, something inbetween is needed, e.g., something that is more computationally efficient but has enough flexibility to apply to the types of field tests that are envisioned for future efforts. Nevertheless, it may be useful to investigate CFD model frameworks to gain a better understanding of the considerable task that is undertaken when attempting to develop such software. Then, one can begin to explore alternate model frameworks, which are reliable, rapid, and robust to simulate meteorology and turbulence in urban environments (e.g., to study atmospheric effects on acoustic propagation or free-space optical communications).

This paper initiates the investigative process by presenting a critical assessment of six CFD model frameworks. Section 2 gives a brief review of the different model simulations of wind flow and the thermal microclimate around single and/or multiple buildings. Two of the selected models account for one or more embedded tree arrays. Additional information (if available) is provided regarding numerical methods, physics/turbulence algorithms, model domain, grid spacing, time-step, runtime, and computer platform. Section 3 discusses some of the difficulties and/or deficiencies with each modeling approach. Section 4 gives a summary and conclusions.

2. Model Survey

The numerical models described in this section were selected via an electronic internet search of the most current literature. Selections were based on accessibility of information regarding model type, numerical methods, physics/turbulence algorithms, grid spacing, time step, model domain, runtime, and computer platform. Table 1 presents a comparison chart for the six CFD models, which contains these kinds of data. The data in table 1 show that the selected CFD models make use of different numerical methods (e.g., finite difference, finite volume, and finite element) to mathematically solve the equation set. Also, the selected CFD models employ combinations of different physics/turbulence approaches [e.g., Reynolds Averaged Navier-Stokes (RANS), large eddy simulation (LES), and kinetic energy—dissipation ($k - \varepsilon$) turbulence models] to resolve the computed fields.

Table1. Comparison of CFD models.

Computational method/ Physics approach	**Author(s)**	**Features**	**Turbulence**	**Grid spacing / Time step**	**Runtime**
3D Finite Difference (Incompressible flow)	Bruse and Fleer (1998)	Multiple buildings; Embedded array of trees	$k-\varepsilon$ model 1.5 order closure	61 x 56 x 25 grids $\Delta x = \Delta y = 5m$; $\Delta z = 4$m; $\Delta t = 10$s	6.0 hrs
3D Finite Difference – RANS (Pseudo-compressible flow)	Wang et al., (2004)	Pedestrian winds around tall buildings	$k-\varepsilon$ model	51 x 163 x 71 grids 200 m x 648 m x 280 m $\Delta x = \Delta y = \Delta z = 4$m; $\Delta t = 0.04$s	($t = 20$ min) (~8.3 hrs)
3D Finite Control Volume (Incompressible flow)	Paterson and Apelt (1989)	Single prismatic building	$k-\varepsilon$ model	Non-uniform staggered grid Steady state	15 min (IBM 3083E)
	Johnson et al., (1997) Herbert et al., (1998)	Urban canyon winds and thermal microclimate (two buildings)	$k-\varepsilon$ model	240 m x 632 m x 100 m 1-2 m grid inside canyon 15-20 m grid outside canyon	45 min. (8 processor super computer)
3D Finite Volume – RANS (Incompressible flow)	Kim and Baik (2004) Baik et al., (2003)	Multiple building array	RNG $k-\varepsilon$ model	Non-uniform staggered grid 101 x 101 x 41 cells 63.1 m x 63.1 m x 28.5 m $\Delta t = 0.05s$	$t = 20$ min (~ 6.7 hrs)
3D Finite Volume – LES (Compressible flow)	Pullen et al., (2004); Boris (2002)	Multiple buildings (Central business district)	MILES model	860 x 580 x 40 grids (Washington DC) 360 x 360 x 55 grids (Chicago) $\Delta x = \Delta y = \Delta z = 6$m; $\Delta t = 0.36$s	8.0 hrs (16 processor super computer)
3D Finite Element – RANS (Incompressible flow)	Calhoun et al., (2004)	Single complex building; Nearby array of trees	similarity–k model	1.0-2.5 x 10^6 grid pts. 400 m x 400 m x 80 m Non-uniform grid (finest grid = 1 m)	~ 1.0 hr (128 processor super computer)

2.1 Three-Dimensional (3-D) Finite Difference Model (Multiple buildings with an embedded array of trees)

The paper given by Bruse and Fleer (*3*) describes a non-hydrostatic, 3-D, microscale, numerical model (called ENVI-met) for surface-plant-air interactions in and around urban structures. The model ENVI-met solves the basic, incompressible, Navier-Stokes equations forward in time via finite difference numerical methods. The main model equations as presented by Bruse and Fleer (*3*) are as follows:

For i = 1,2,3

$$\frac{\partial u}{\partial t} + u_i \frac{\partial u}{\partial x_i} = -\frac{\partial p'}{\partial x} + K_m \left(\frac{\partial^2 u}{\partial x_i^2} \right) + f\left(v - v_g\right) - S_u \ , \tag{1}$$

$$\frac{\partial v}{\partial t} + u_i \frac{\partial v}{\partial x_i} = -\frac{\partial p'}{\partial y} + K_m \left(\frac{\partial^2 v}{\partial x_i^2} \right) - f\left(u - u_g\right) - S_v \ , \tag{2}$$

$$\frac{\partial w}{\partial t} + u_i \frac{\partial w}{\partial x_i} = -\frac{\partial p'}{\partial z} + K_m \left(\frac{\partial^2 w}{\partial x_i^2} \right) + g \frac{\theta(z)}{\theta_{ref}(z)} - S_w \ , \tag{3}$$

$$\frac{\partial u}{\partial x} + \frac{\partial v}{\partial y} + \frac{\partial w}{\partial z} = 0 \ , \tag{4}$$

$$\frac{\partial \theta}{\partial t} + u_i \frac{\partial \theta}{\partial x_i} = K_h \left(\frac{\partial^2 \theta}{\partial x_i^2} \right) + Q_h \ , \tag{5}$$

and

$$\frac{\partial q}{\partial t} + u_i \frac{\partial q}{\partial x_i} = K_q \left(\frac{\partial^2 q}{\partial x_i^2} \right) + Q_q \ . \tag{6}$$

Here, t is the independent variable time, u, v, and w are the mean wind velocity components, u_i is the *i-component* of the wind velocity vector ($u_1 = u$, $u_2 = v$, $u_3 = w$), and x_i is the *i-component* of the position vector ($x_1 = x$, $x_2 = y$, $x_3 = z$). In addition, p' is the local pressure perturbation, K_m, K_h, and K_q are the turbulent exchange coefficients for momentum, heat, and moisture,

respectively, f (= 10^4 sec^{-1}) is the Coriolis parameter, u_g and v_g are the geostrophic wind components, θ is potential temperature, and q is specific humidity. In equations 1 through 3, the source/sink terms (S_u, S_v, and S_w) describe the loss of wind speed due to drag forces from vegetation. In equations 5 and 6, Q_h and Q_q are the source/sink terms for atmospheric heat and moisture, respectively. Two additional equations describe the 1.5 order closure, $k-\varepsilon$ turbulence sub-model (*4*,*5*). They are as follows: For i = 1,2,3

$$\frac{\partial E}{\partial t} + u_i \frac{\partial E}{\partial x_i} = K_E \left(\frac{\partial^2 E}{\partial x_i^2} \right) + \Pr - Th + Q_E - \varepsilon \ , \tag{7}$$

and

$$\frac{\partial \varepsilon}{\partial t} + u_i \frac{\partial \varepsilon}{\partial x_i} = K_\varepsilon \left(\frac{\partial^2 \varepsilon}{\partial x_i^2} \right) + c_1 \frac{\varepsilon}{E} \Pr - c_3 \frac{\varepsilon}{E} Th - c_2 \frac{\varepsilon^2}{E} + Q_\varepsilon \ . \tag{8}$$

Here, E is the local turbulence (i.e., turbulent kinetic energy (t.k.e.), where $E = k = \overline{u_i u_i}/2$), ε is the t.k.e. dissipation rate, *Pr* is the mechanical production of t.k.e., *Th* is the buoyancy production of t.k.e., K_E and K_ε are exchange coefficients, Q_E and Q_ε are source/sink terms, and c_1, c_2, and c_3, are numerical constants.

To solve the combined advection–diffusion equations, the alternating directions implicit method (ADI) and an upstream advection scheme is used. Dynamic pressure is removed from the equations of motion and calculated separately from the Poisson equation. The model can simulate wind field modifications around solid boundaries like walls as well as modifications through porous media like trees. The ENVI-met model contains sub-models for the mean wind flow, temperature and humidity, turbulence and kinetic energy processes, radiative fluxes, soil and vegetation interactions, and ground surface and wall(s) interactions. Bruse and Fleer (*3*) provide an interesting case study to show changes in local wind flow and calculated temperature fields through a typical central business district (figures 1 through 3).

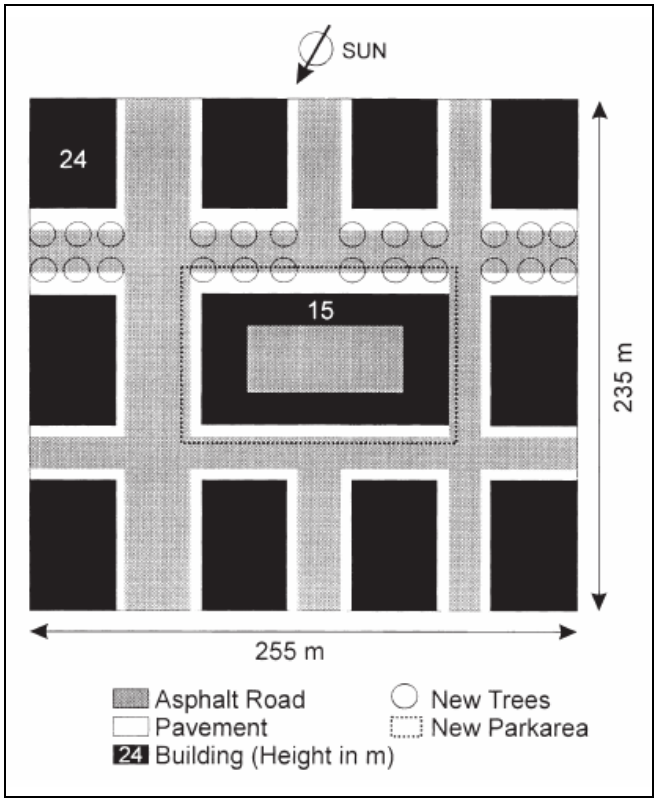

Figure 1. Schematic of the building geometry for an ENVI-met model case study. Outer buildings are 24 m in height and center buildings are 15 m. Some trees are planted along the upper street canyon (from Bruse and Fleer [*3*]).

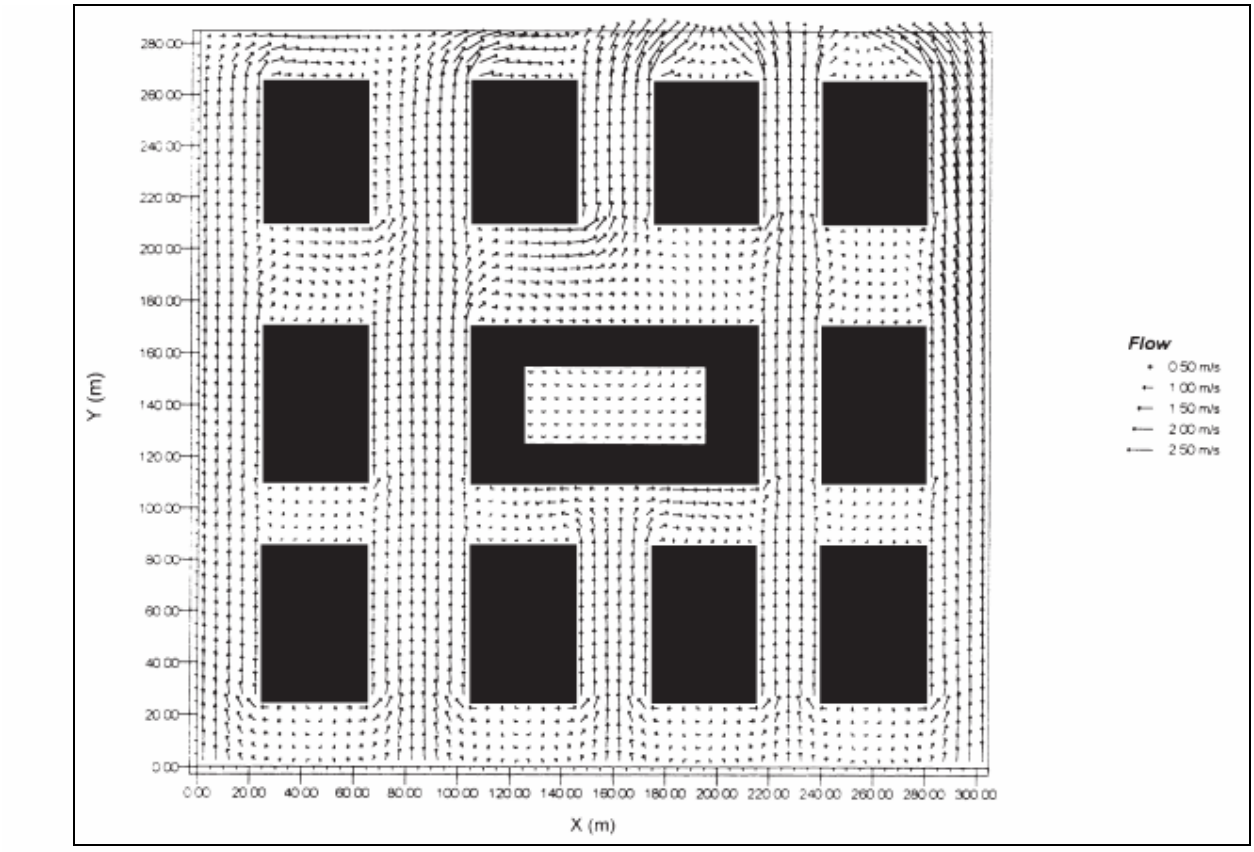

Figure 2. An ENVI-met model calculation of the horizontal wind field at z = 2 m, where the initial wind direction is $\theta = 90°$ (from Bruse and Fleer [*3*]).

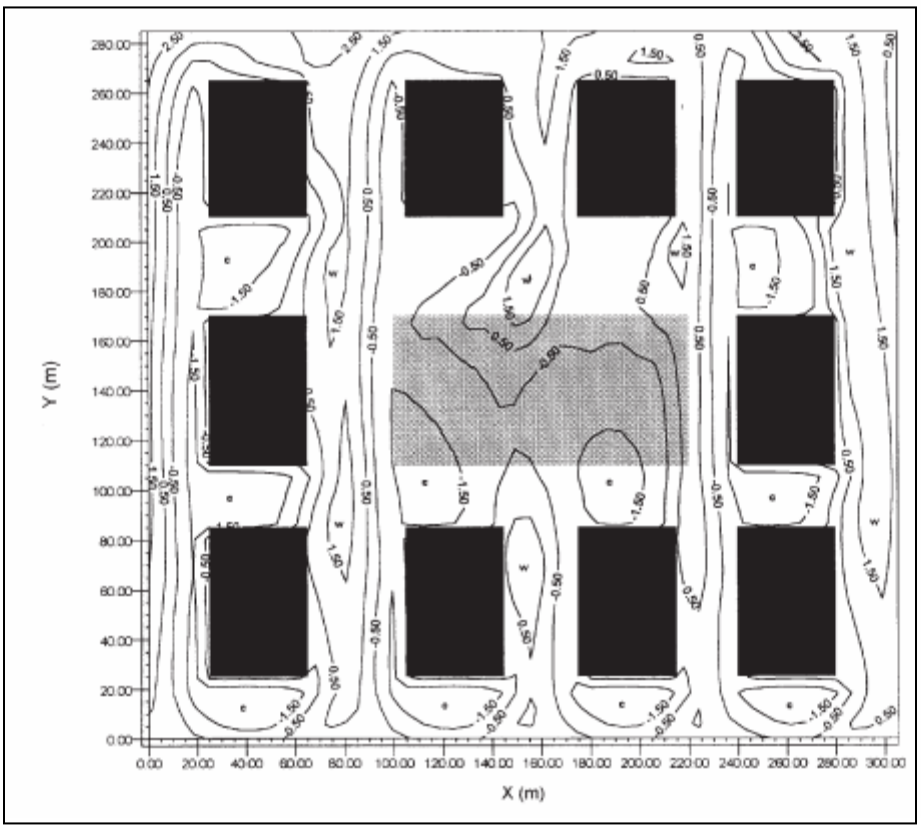

Figure 3. An ENVI-met model calculation of the (normalized) temperature field at z = 2 m. The grey area indicates a central park with trees. Different surface temperatures result due to shading by buildings and trees. These effects produce a pattern of warmer (w) or colder (c) areas than the average reference temperature at the same level (from Bruse and Fleer [*3*]).

The main time step for the ENVI-met model is $\Delta t = 10$ s. Smaller time steps are used for the k–ε turbulence model. Even grid spacing ($\Delta x = \Delta y = 5$ and $\Delta z = 4$m) is used in each direction, however, the lowest grid cell above ground is split into five cells with size $\Delta z_g = 0.2\Delta z$ to increase accuracy in calculating surface processes, e.g., the surface radiation and energy budget. In the case study described above, the ENVI-met model contained 61 x 56 x 25 grid points (300 x 275 x 96 m). The model calculation takes approximately 6 hours to resolve the computed fields.

2.2 Three-Dimensional (3-D) Finite Difference Model – RANS (Pedestrian winds around tall buildings)

Wang et al., (*6*) describe a 3-D, microscale, wind flow model [called PUMA (Peking University Model of Atmospheric Environment)] to calculate pedestrian winds around tall buildings. The PUMA model is based on the Reynolds Averaged Navier-Stokes (RANS) equations, where the atmosphere is assumed to be neutral, i.e., without thermal effects. (Note that implementing

energy equations, heat flux equations, source/sink terms, and buoyancy effects frequently demand additional computer time and resources, which the developer may not consider necessary to achieve acceptable model results). The main model equations as presented by Wang et al., (*6*) are as follows: For $i,j = 1,2,3$

$$\frac{\partial u_i}{\partial x_i} = 0\,, \tag{9}$$

$$\frac{\partial u_i}{\partial t} + u_j \frac{\partial u_i}{\partial x_j} = -\frac{1}{\rho}\frac{\partial p}{\partial x_i} - \frac{\partial}{\partial x_j}\left(R_{ij}\right), \tag{10}$$

where u_i is the mean velocity component in the i-th direction, ρ is the air density, and p is the fluctuating pressure. The Reynolds stress, $R_{ij} = \overline{u_i u_j}$, represents the effects from turbulence.

Familiar summation notation is used in equations 9 and 10 (and elsewhere in this section of the report). Tunick (*7*) provides several useful examples to demonstrate how the complete equation set can be extracted by expanding the summation indices.

The wind flow equation is integrated forward in time via finite differencing, although the virtual compress (pseudo-compressible flow) method as described by Chorin (*8*) is adopted to solve for the pressure field. The Reynolds stress (turbulence) is solved via a modified k - ε turbulence model as described by Jones and Lauder (*9*). The equations for the t.k.e. (k) and its dissipation (ε) as presented by Wang et al., (*6*) are as follows: Using regular summation notation for $i,j = 1,2,3$

$$\frac{\partial k}{\partial t} + u_j \frac{\partial k}{\partial x_j} = -R_{ij}\frac{\partial u_i}{\partial x_j} + \frac{\partial}{\partial x_i}\left(\frac{K}{\sigma_k}\frac{\partial k}{\partial x_i}\right) - \varepsilon\,, \tag{11}$$

and

$$\frac{\partial \varepsilon}{\partial t} + u_j \frac{\partial \varepsilon}{\partial x_j} = -c_{\varepsilon 1}\frac{\varepsilon}{k}R_{ij}\frac{\partial u_i}{\partial x_j} + \frac{\partial}{\partial x_i}\left(\frac{K}{\sigma_\varepsilon}\frac{\partial \varepsilon}{\partial x_i}\right) - c_{\varepsilon 2}\varepsilon^2/k\,, \tag{12}$$

where K is the turbulent viscosity and σ_k, σ_ε, $c_{1\varepsilon}$, and $c_{2\varepsilon}$ are numerical constants.

For the case study presented in Wang et al., (*6*), the computational domain is 200 m x 648 m x 280 m with even grid spacing in all directions (i.e., $\Delta x = \Delta y = \Delta z = 4$m). The total number of grid points is 51 x 163 x 71 and the time step is $\Delta t = 0.04$ s. Although not stated directly in their paper, a $t = 20$ minute simulation would take approximately 8.3 hours to complete. Figure 4 shows an example PUMA model calculation of the horizontal wind field at z = 2m.

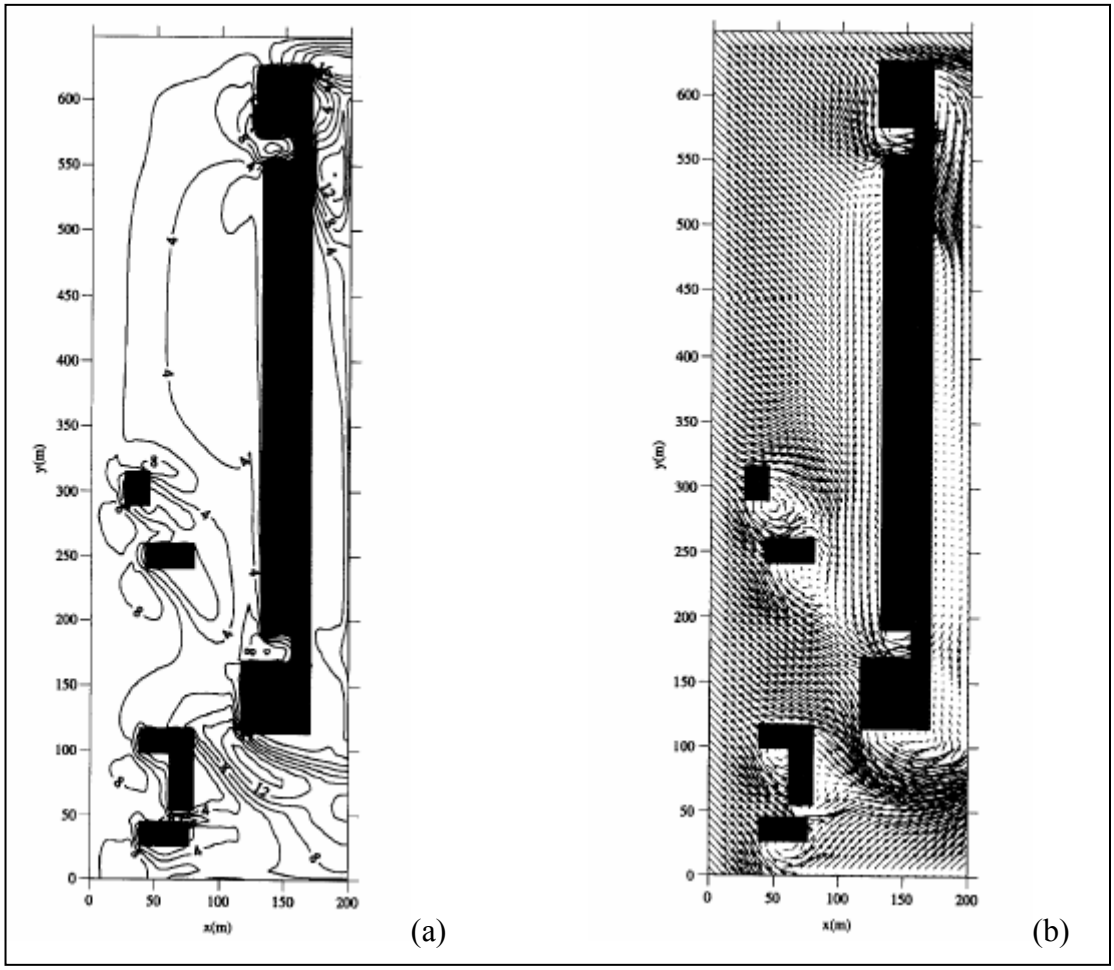

Figure 4. A PUMA model calculation of the horizontal wind field at z =2m, i.e., wind velocity contours (a) and wind velocity vectors (b) (from Wang et al. [*6*]).

2.3 Three-Dimensional (3-D) Finite Control Volume Model (Single building and/or urban street canyon)

Paterson and Apelt (*10*) describe a 3-D, flat terrain, steady-state, finite difference model (called CITY) for a single prismatic building[1]. The CITY model time averages the (Navier-Stokes) Reynolds equation and the continuity equation to compute the mean wind fields. The CITY model contains six equations and the following six unknowns; the turbulent kinetic energy ($k = \overline{u_i u_i}/2$) and its dissipation (ε), the three mean velocity components ($u_1 = u$, $u_2 = v$, $u_3 = w$),

[1] Prismatic is defined as blocks with well-defined vertical faces, where the vertical axes are much longer than the horizontal axes (http://www.onelook.com).

and the augmented pressure (P). As presented by Paterson and Apelt (*10*), the main model equations are as follows: Using regular summation notation for i,j = 1,2,3

$$u_j \frac{\partial k}{\partial x_j} = \frac{\partial}{\partial x_i}\left(\frac{v_t}{\sigma_k}\frac{\partial k}{\partial x_j}\right) + v_t\left(\frac{\partial u_i}{\partial x_j} + \frac{\partial u_j}{\partial x_i}\right)\frac{\partial u_i}{\partial x_j} - \varepsilon\,, \tag{13}$$

and

$$u_j \frac{\partial \varepsilon}{\partial x_j} = \frac{\partial}{\partial x_i}\left(\frac{v_t}{\sigma_\varepsilon}\frac{\partial \varepsilon}{\partial x_j}\right) + c_1 c_\mu k\left(\frac{\partial u_i}{\partial x_j} + \frac{\partial u_j}{\partial x_i}\right)\frac{\partial u_i}{\partial x_j} - c_2\frac{\varepsilon^2}{k}\,, \tag{14}$$

$$u_j \frac{\partial u_i}{\partial x_j} = \frac{\partial}{\partial x_i}\left(v_t \frac{\partial u_i}{\partial x_j}\right) - \frac{\partial P}{\partial x_i}\,, \tag{15}$$

and

$$\frac{\partial u_j}{\partial x_j} = 0\,. \tag{16}$$

Here, v_t is the turbulent viscosity and σ_k, σ_ε, c_1, c_2, and c_μ are numerical constants.

The above equations are discretized by the finite control volume technique, i.e., partial differential equations are integrated over appropriate control volumes on a staggered grid to obtain the difference equations. Here, hybrid upwind differencing is used. The grid is a staggered grid that expands geometrically away from building faces. The method by which the pressure is calculated is known as SIMPLE, i.e., Semi-Implicit Method for Pressure Linked Equations (*11*). The CITY model makes use of a $k-\varepsilon$ turbulence scheme to resolve the Reynolds stress. The resulting algebraic equations are solved by a 3-D version of the ADI (alternating direction implicit) procedure in which three sweeps of the solution domain (one in each of the coordinate directions) are done in each iteration. Convergence takes about a hundred iterations and requires about 15 minutes on an IBM 3083E computer. Figure 5 shows an example of the wind velocity vectors computed from the CITY model.

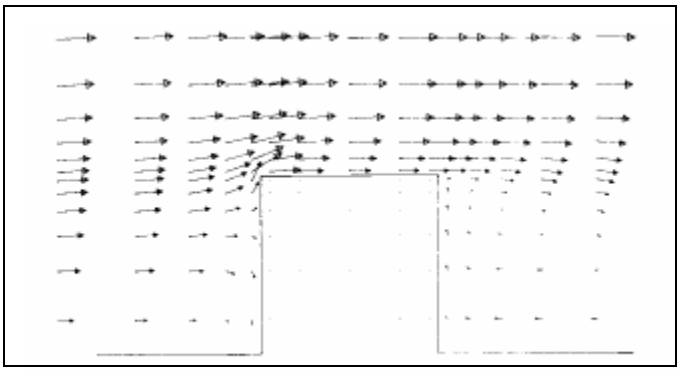

Figure 5. Example wind velocity vectors computed from the CITY model (from Paterson and Apelt [*10*]).

Similarly, Johnson et al., (*12*), Herbert et al., (*13*) and Herbert and Herbert (*14*) describe a coupled urban wind flow model (CITY) and a two-dimensional (2-D) thermal microclimate model (called SCALAR and ENERBAL) for city canyons, i.e., two buildings. The wind flow model CITY was developed by Paterson and Apelt (*10*) (as described above). For the coupled urban model, the steady state wind field is computed separately and is maintained throughout the temperature simulation. The atmospheric diffusion equation in the SCALAR model as described by Johnson et al., (*12*) is as follows: Using regular summation notation for i = 1,2,3

$$\frac{\partial T}{\partial t} + u_i \frac{\partial T}{\partial x_i} = \frac{\partial}{\partial x_i}\left(K_h \frac{\partial T}{\partial x_i} \right) + S \tag{17}$$

where T is the air temperature at a point in space, K_h is eddy diffusivity for heat, and S (x, y, z, t) is the source/sink term. Here, only advection (by the wind field) and diffusion components are considered.

In addition, the coupled urban model makes the simplifying assumption that the buildings on each side of the urban canyon are of equal height and length, and that the buildings are rectangular in shape, and that each surface is constructed of a homogeneous material. The SCALAR and ENERBAL models simulate the 2-D temperature field within and around an urban canyon as a function of the time of day, time of year, the wind field, location of the city, the canyon orientation, the construction materials of the buildings and street, and as a result, the heat fluxes at the building and other surfaces. Figure 6 shows a schematic of the geometry for the coupled urban wind flow and thermal microclimate model.

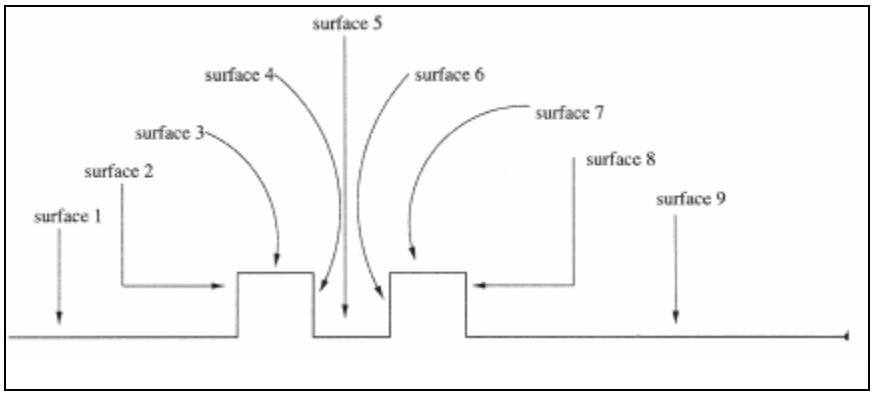

Figure 6. A schematic (geometry) for the coupled wind flow and urban thermal microclimate model described in Herbert et al., (*13*).

The coupled urban model domain is divided into non-overlapping contiguous control volumes (e.g., 240 m x 632 m x 100 m). For computational efficiency, control volumes are selected to be smaller close to the ground and within the canyon (1-2 m grid), and larger above the buildings and outside the canyon (15-20 m grid). The temperature in a given volume of air is treated as a passive scalar, which does not affect the wind flow. Hence, the coupled urban model assumes that the effect of buoyancy is negligible when compared to the temperature dispersion created by the wind field. As described by Herbert et al., (*13*), the coupled urban model is implemented on a Cray Y-MP8E, 8-processor super computer. On that platform, the steady-state wind field takes about 25 minutes to resolve and the combined thermal microclimate model takes an additional 20 minutes to simulate a 48-h period. Figure 7 shows an example result from the coupled wind flow and thermal microclimate model, i.e., predicted air temperatures (°C) across an urban canyon at 1 p.m. (on March 15).

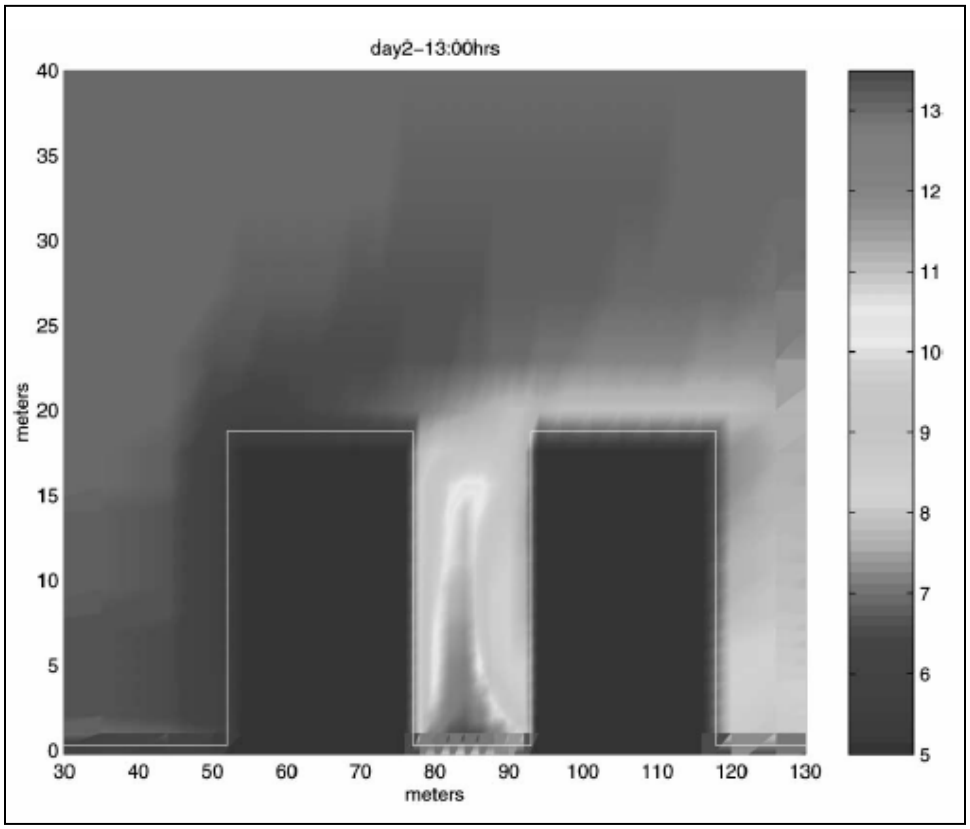

Figure 7. Example results from the coupled wind flow and thermal microclimate model, i.e., predicted air temperatures (°C) across an urban canyon at 1 p.m. on 15 March (from Herbert and Herbert [*14*]).

2.4 Three Dimensional (3-D) Finite Volume – RANS (Multiple building array)

Kim and Baik (*15*) and Baik et al., (*16*) describe their 3-D, RANS, CFD model with the Renormalization Group (RNG) k - ε turbulence scheme (*17*) to investigate non-hydrostatic, non-rotating, incompressible wind flows in complex urban environments. Their model is based on the earlier works of Kim and Baik (*18*) and Baik and Kim (*19*). The governing equation set is solved on a non-uniform, staggered grid system (*20*) using a finite volume method with the semi-implicit method for pressure-linked equation (SIMPLE) algorithm (*11*). Smaller grid sizes near buildings and larger grid sizes away from buildings are used to (more efficiently) resolve flow and dispersion fields. The model equations as presented by Kim and Baik (*15*) are as follows: Using regular summation notation for i,j = 1,2,3

$$\frac{\partial u_i}{\partial t} + u_j \frac{\partial u_i}{\partial x_j} = -\frac{1}{\rho}\frac{\partial P^*}{\partial x_i} + \nu \frac{\partial^2 u_i}{\partial x_j \partial x_j} - \frac{\partial}{\partial x_j}\left(\overline{u_i u_j}\right), \tag{18}$$

$$\frac{\partial u_i}{\partial x_i} = 0\,, \tag{19}$$

$$\frac{\partial k}{\partial t} + u_j \frac{\partial k}{\partial x_j} = -\overline{u_i u_j} \frac{\partial u_i}{\partial x_j} + \frac{\partial}{\partial x_j}\left(\frac{K_m}{\sigma_k}\frac{\partial k}{\partial x_j}\right) - \varepsilon\,, \tag{20}$$

and

$$\frac{\partial \varepsilon}{\partial t} + u_j \frac{\partial \varepsilon}{\partial x_j} = -C_{\varepsilon 1}\frac{\varepsilon}{k}\overline{u_i u_j}\frac{\partial u_i}{\partial x_j} + \frac{\partial}{\partial x_J}\left(\frac{K_m}{\sigma_\varepsilon}\frac{\partial \varepsilon}{\partial x_J}\right) - C_{\varepsilon 2}\varepsilon^2 / k - R \quad , \tag{21}$$

where the Reynolds stress is $\overline{u_i u_j}$, P* is the deviation of pressure from its reference value, and *R* is an extra strain term, i.e.,

$$R = \frac{C_\mu \eta^3 (1 - \eta/\eta_0)\varepsilon^2}{(1 + \beta_0 \eta^3)k}\,, \tag{22}$$

where

$$\eta = \frac{k}{\varepsilon}\left[\left(\frac{\partial u_i}{\partial x_j} + \frac{\partial u_j}{\partial x_i}\right)\frac{\partial u_i}{\partial x_j}\right]^{1/2}. \tag{23}$$

Here, σ_k, σ_ε, $C_{1\varepsilon}$, $C_{2\varepsilon}$, C_μ, η_0, and β_0 are numerical constants (*18*).

In the case study described by Kim and Baik (*15*), a group of buildings is embedded across 101 x 101 x 41 cells. The dimension of the smallest cell is 0.3 m x 0.3 m x 0.3 m, which is situated at the edges of the buildings. The largest cell dimensions are 1.8 m x 1.8 m x 1.8 m. The model domain is 63.1 m x 63.1 m x 28.5 m. The time step used in this case is $\Delta t = 0.05s$. The computer model is integrated up to t = 20 minutes (e.g., ~6.7 hours runtime). However, Kim and Baik (*15*) indicate that a quasi-steady state in the wind flow field is established after t = 5-7 minutes. Figure 8 shows example model results from this calculation.

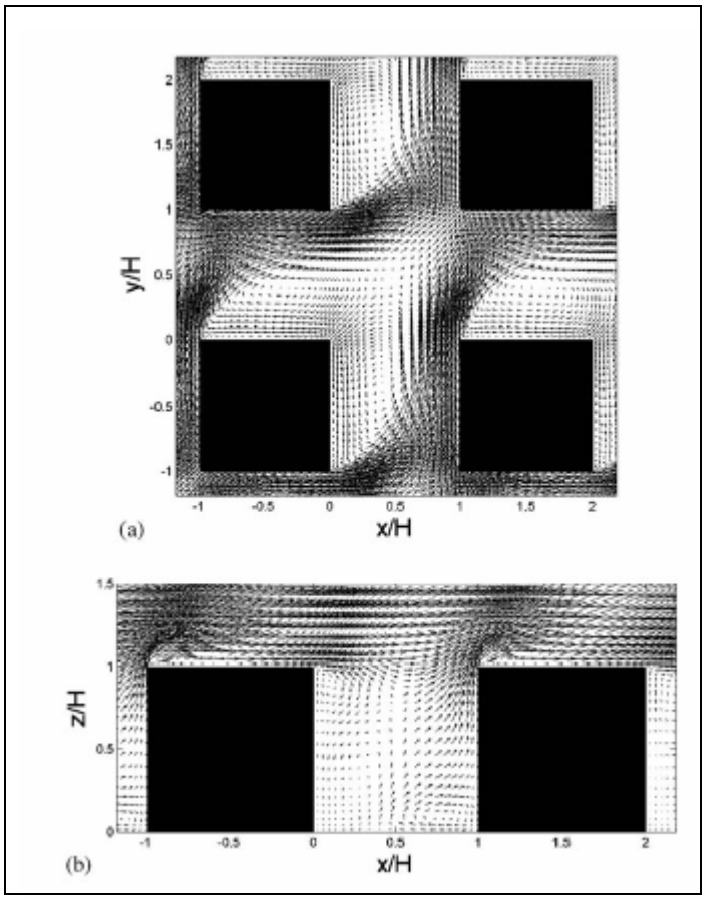

Figure 8. The wind vector fields from the CFD model of Kim and Baik (*15*) at (a) z/H = 0.5 and (b) y/H = -0.75 for the case where the initial wind direction is $\theta = 45°$.

2.5 Three Dimensional (3-D) Finite Volume – LES (Multiple buildings; Central business district)

Pullen et al., (*21*) and Boris (*22*) describe their 3-D, finite volume, CFD model (called FAST3D-CT) with the monotone integrated large eddy subgrid (MILES) turbulence model (*23*,*24*) embedded to solve the high Reynolds number, time-dependent, Navier–Stokes equations for mass, momentum, potential temperature, and contaminants. The time integration is second-order accurate and has been adapted for fast execution with very complex geometry. The CFD algorithms solve for slow but compressible flow. (Note: While most atmospheric boundary layer models assume incompressible flow, some developers incorporate compressible flow features when, for example, detailed representation of thermal (eddy) updrafts and downdrafts are desired [*25*].) In addition, the model incorporates a complex finite volume algorithm for detailed building and city aerodynamics. The model physics implemented to compute the urban thermal microclimate includes solar heating of surfaces based on land-use data tables. The model considers shadows from buildings and trees (depending on the time of day) and heat transfer

from building sides and tops (for both daytime and nighttime cases). Buoyancy is included in the potential temperature calculation. (Note that a list of the governing equations for the FAST3D-CT model was not readily available).

Pullen et al., (*21*) presented contaminant diffusion simulations for Washington D.C. and Chicago, wherein the FAST3D-CT model's horizontal and vertical grid spacing was $\Delta x = \Delta y = \Delta z = 6$m. The computational time-step was $\Delta t = 0.36$s. The model grid embedded a 1-m resolution building database. The grid dimensions were 860 x 580 x 40 levels for Washington D.C. and 360 x 360 x 55 levels for Chicago. Typically, the FAST3D-CT model simulation of a 10 km^2 area at 6 m resolution takes 8 hours on a 16 processor super computer. Figure 9 shows a contour plot of wind velocities for air flowing across the Washington, DC mall (from Boris [*22*]).

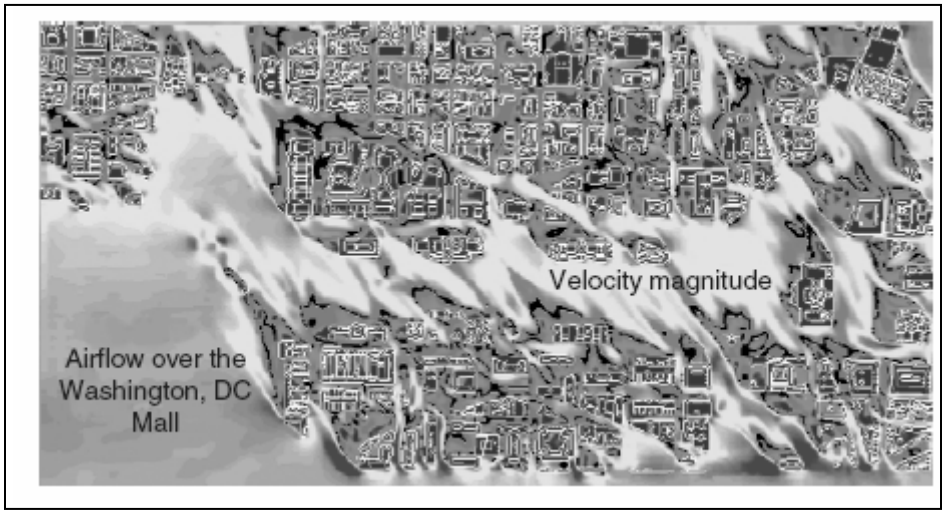

Figure 9. A contour plot of wind velocities for air flowing across the Washington, DC mall (from Boris [*22*]).

2.6 Three Dimensional (3-D) Finite Element – RANS (Single complex building surrounded by a complex array of trees)

Calhoun et al., (*26*) present their 3-D, RANS, CFD model (called FEM3) to simulate wind flow and momentum around a single complex building surrounded by a complex array of trees. In their study, numerical data are compared to field measurements. The wind flow was assumed to be neutral, i.e., cloudy, morning, or higher-wind conditions. The turbulence model used is the similarity–*k* turbulence model, wherein the turbulent fluxes are parameterized as proportional to gradients of mean variables. Canopy effects (e.g., a line of eucalyptus trees to the east of the building) were modeled with the addition of a drag term in the momentum equations, following Yamada (*27*). The FEM3 code uses a finite-element method (as discussed by Chan et al., [*28*])

and has been adapted for use on massively parallel computer platforms. The governing equations for the FEM3 model as presented by Chan et al., (*28*) are as follows:

$$\frac{\partial\left(\rho\vec{u}\right)}{\partial t}+\rho\vec{u}\nabla\vec{u}=-\nabla p+\nabla\cdot\left(\rho K^{m}\cdot\nabla\vec{u}\right)+\left(\rho-\rho_{h}\right)\vec{g}\,, \tag{24}$$

$$\nabla\cdot\left(\rho\vec{u}\right)=0\,, \tag{25}$$

$$\frac{\partial\theta}{\partial t}+\vec{u}\nabla\theta=\frac{1}{\rho C_{P}}\nabla\cdot\left(\rho C_{P}K^{\theta}\cdot\nabla\theta\right)+\frac{C_{PN}+C_{PA}}{C_{P}}\left(K^{\omega}\cdot\nabla\omega\right)\cdot\nabla\theta\,, \tag{26}$$

$$\frac{\partial\omega}{\partial t}+\vec{u}\nabla\omega=\frac{1}{\rho}\nabla\cdot\left(\rho K^{\omega}\cdot\nabla\omega\right), \tag{27}$$

and

$$\rho=\frac{PM}{RT}=\frac{P}{RT\left(\dfrac{\omega}{M_{N}}+\dfrac{1-\omega}{M_{A}}\right)}\,. \tag{28}$$

Here, $\vec{u}=\left(u,\ v,\ w\right)$ is the wind velocity, ρ is the density of the mixture (e.g., dry air and water vapor), p is the pressure deviation from an isothermal atmosphere at rest with corresponding density ρ_h, $\vec{g}$ is the acceleration due to gravity, θ is the potential temperature deviation from adiabatic, ω is the mass fraction of the species (e.g., water vapor or dispersed contaminant), K^m and K^θ, K^ω are the eddy diffusivity tensors for momentum, energy, and the dispersed species, respectively, and C_{PN}, C_{PA}, and $C_p = \omega C_{PN} + (1 - \omega)C_{PA}$ are the specific heats for the species, air, and the mixture, respectively. In the equation of state [equation 26], P is the absolute pressure, R is the universal gas constant, M_N and M_A are the molecular weights of the species and air, and T is the absolute temperature.

Figure 10 shows the building geometry and surrounding array of trees for the case study described by Calhoun et al., (*26*). Figure 11 shows an example result (modeled wind vectors versus experimental data) for the complex (building and tree) geometry shown in figure 10. Background momentum fields are also shown. Here, approximately 1.0-2.5 x 10^6 grid points were used. Grid stretching allowed the finest grid spacing near the building to be approximately 1 m. The model domain was 400 m x 400 m x 80 m. The model simulation took approximately 1 hour to complete on a 128 processor super computer (i.e., the advanced simulation and computing program [ASCI] Blue-Pacific machine).

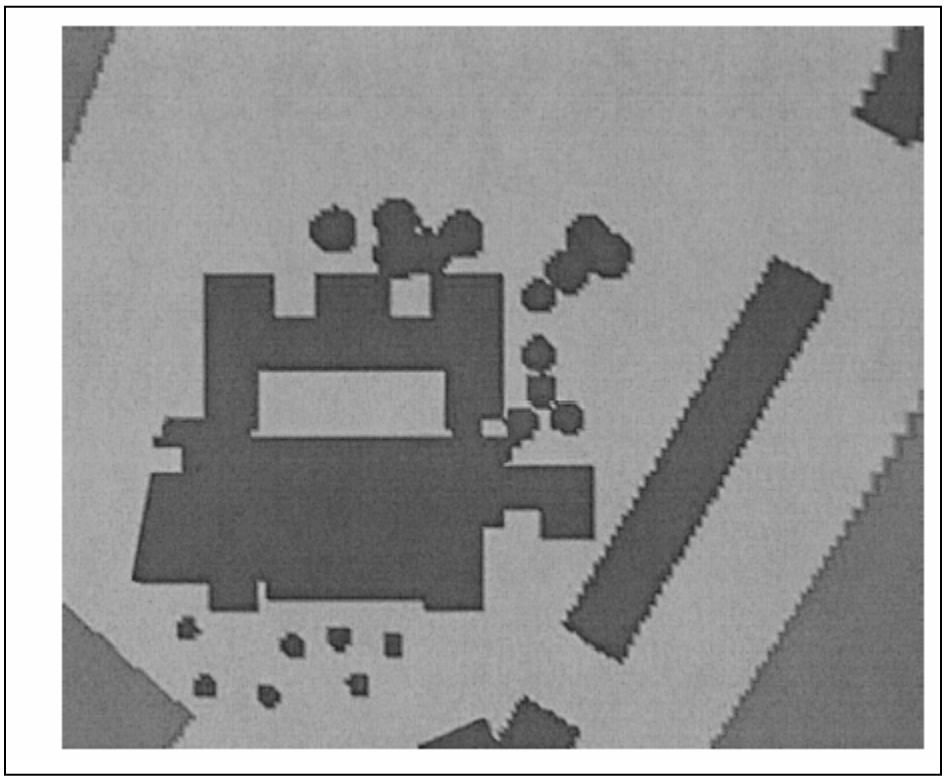

Figure 10. A schematic of the building geometry for the case study described by Calhoun et al., (*25*). The circular and the rectangular shaded regions are tree locations surrounding the building.

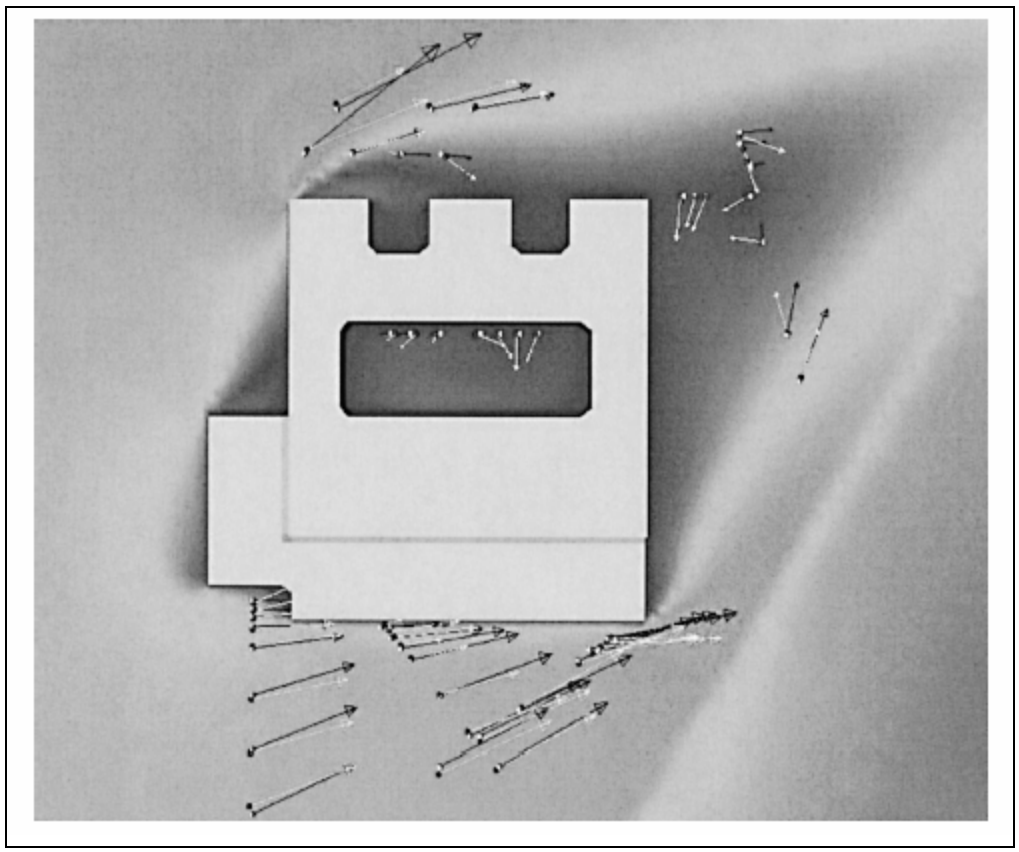

Figure 11. Example results (modeled wind vectors versus experimental data) from the FEM3 code. White vectors are experimental data and black vectors are model data. Background shading represents modeled momentum, where low momentum is dark and high momentum is lighter (from Calhoun et al., [*25*]).

3. Discussion

This section outlines some of the main properties the modeling frameworks summarized above, to include a discussion of difficulties and/or deficiencies associated with each approach.

3.1 Finite Difference Method

Finite difference methods have been around the longest for numerical solution of partial differential equations (29). Some researchers consider finite difference methods to be the easiest, most flexible, and most effective approach for simple geometries. Finite difference methods easily allow for higher-order schemes over regular grids. Variable grid can also be implemented in a straightforward manner to allow for better distribution of grid points, which may help to better resolve important atmospheric scales and processes (*30*). In contrast,

numerical simulation of wind flow through complex geometries, such as those found in urban settings, may be quite difficult via finite difference methods.

Nevertheless, one begins by putting the conservation equation (e.g., mass conservation, advection-diffusion, etc.) in differential form. Then, at each grid point, the partial derivatives are replaced by approximations (e.g., forward, backward, or central differences) in terms of the nodal value of the functions. The result is one algebraic equation per grid node, in which the variable value at that and several neighboring nodes appear as unknowns (*29*).

As an example, the conservation (simplified Navier-Stokes) equation to describe the mean concentration (advection-diffusion) of a scalar $\overline{C}$ can be written as follows:

$$\frac{\partial \overline{C}}{\partial t} = -\overline{u}\frac{\partial \overline{C}}{\partial x} - \frac{\partial \overline{w'C'}}{\partial z}, \tag{29}$$

where t is the independent variable time, $\overline{u}$ is the mean longitudinal component of the wind velocity, x is range, z is height above ground, and $\overline{w'C'}$ is the mean scalar flux. The flux-gradient assumption (*31*) suggests that

$$-\overline{w'C'} = K\frac{\partial \overline{C}}{\partial z}, \tag{30}$$

Where K is the scalar (eddy) diffusivity. Combining equations 29 and 30 yields,

$$\frac{\partial \overline{C}}{\partial t} = -\overline{u}\frac{\partial \overline{C}}{\partial x} + K\frac{\partial^2 \overline{C}}{\partial z^2}. \tag{31}$$

In discretized form, this simple model can be solved forward in time using an explicit finite differencing scheme for uniform grid, i.e.,

$$C_{i,j}^{n+1} = C_{i,j}^{n} + \Delta t\left[-u_{i,j}\frac{C_{i,j}^{n} - C_{i-1,j}^{n}}{\Delta x} + K\frac{C_{i,j+1}^{n} - 2C_{i,j}^{n} + C_{i,j-1}^{n}}{(\Delta z)^2}\right], \tag{32}$$

where i and j are the indices for the horizontal and vertical grid, respectively, and n is the time-step. For an explicit scheme, the time-step should be small to satisfy the stability criterion, $2K\Delta t/(\Delta z)^2 < 1$, as discussed by Press et al., (*32*) (page 838). Otherwise, for larger time-steps, the numerical scheme would be unstable and the model would not produce viable results.

3.2 Finite Volume Method

At the start, the finite volume method uses the integral form of the conservation equations. As an example, the integral form of a (simplified) conservation equation to describe the mean concentration of a scalar $\overline{C}$ can be written as

$$\int_V C dV + \int_S C\vec{u}\cdot\vec{n}\ dS = \int_S K\nabla C\cdot\vec{n}\ dS \tag{32}$$

where $\int_V$ is a volume integral, $\int_S$ is a surface integral, $\vec{n}$ is the normal vector to the surface of the cell, and ∇ is the (finite volume) divergence operator (*33*). Here, finite volumes (or finite control volumes) are used to discretize the equation set.

With the finite volume method the model domain (space) is broken up into a finite number of contiguous volumes or cells and the conservation equations are applied to each. Staggered grid is often implemented wherein cell centers are indexed j-1, j, and j+1 and cell edges are labeled j-1/2 and j+1/2. In this manner, some variables, e.g., mass and energy, are evaluated at volume centers while momentum is evaluated at the volume edges. Interpolation is used to compute the cell edge (surface) values in terms of the cell center (nodal) values. Surface and volume integrals are approximated using suitable numerical integration techniques, e.g., Newton-Cotes formulas (*29*). To its advantage, finite volume methods can be applied to any type of grid, to include complex geometries. The grid only defines cell boundaries and need not be related to a structured coordinate system. Nevertheless, the selection of uniform, non-uniform, or staggered grid will have a significant effect on the calculation of certain variables. For example, implementing a staggered grid may be quite effective for pressure calculations around different building geometries, but could create complications for deriving wind fields in similar environments (*25*). Also, with a staggered grid, indexing is more complicated.

3.3 Finite Element Method

The finite element method is similar to the finite volume method in that the model domain is broken up into a finite number of cells (which are most often non-uniform and unstructured) and the integral conservation equations are applied to each. In 2-D, the cells are usually triangles or quadrilaterals, while in 3-D tetrahedral or hexahedra are often applied. The distinguishing feature of a finite element model is that the conservation equations are multiplied by a weighting function before they are integrated over the entire domain (*29*). An important advantage of finite element methods is the ability to solve problems involving complex geometries. Grids can be easily refined by simply subdividing the individual elements. The disadvantage of finite element methods, as mentioned above, is that with unstructured grids, indexing is more complicated. Also, with finite element methods (computationally) efficient numerical solution techniques are often more difficult to find. Nevertheless, some researchers find that finite element methods provide a greater flexibility to model complex geometries than either finite difference or finite volume methods (*34*).

Finally, different physics/turbulence algorithms require different kinds and amounts of computer resources. For example, Calhoun et al., (*26*) stated that their RANS approach used about an order of magnitude less c.p.u time than a similar LES approach. While they found certain advantages in using RANS over LES methods, nevertheless, such models require intensive computing capabilities (even if only for calculation of the mean field variables).

4. Summary and Conclusions

This paper presented a critical assessment of six CFD models. The paper was derived from a survey of current numerical frameworks to simulate wind flow and the thermal microclimate around single and/or multiple buildings. This study describes a few complex CFD approaches in order to better understand the enormous task to develop such software. CFD model summaries included information on embedded physics/turbulence algorithms, model domain, grid spacing, time-step, runtime, and computer platform.

This paper showes that computer simulations of wind flow and temperatures in urban areas have most often been achieved via intricate and computationally intensive CFD codes. The paper provides an illustrative overview of current data on this important topic. As a result, it is anticipated that the present study will provide much useful information, from which to initiate several new modeling efforts. For example, it may be advantageous now to explore alternate model frameworks, e.g., those that are more computationally efficient yet flexible enough for the types of future military applications envisioned.

Literature Cited

1. Blocken, B.; Carmeliet, J. Pedestrian wind environment around buildings: Literature review and practical examples. *Journal of Thermal Env. & Bldg. Sci*. **2004**, *28*, 107–159
2. Vardoulakis, S.; Fisher, B.E.A.: Pericleous, K.; Gonzolelz-Flescam, N. Modelling air quality in street canyons: a review. *Atmospheric Environment* **2003**, *37*, 155–182.
3. Bruse, M.; Fleer, H. Simulating surface–plant–air interactions inside urban environments with a three dimensional numerical model. *Environmental Modelling and Software* **1998**, *13*, 373–384.
4. Mellor, G. L. Analytic Prediction of the Properties of Stratified Planetary Surface Layers. *Journal of Atmospheric Science* **1973**, *30*, 1061–1069.
5. Mellor, G. L.; Yamada, T.A.Yamada, Hierarchy of Turbulence Closure Models for Planetary Boundary Layer. *Journal of Atmospheric Science* **1974**, *31*, 1791–1806.
6. Wang, B. M.; Liu, H. Z.; Chen, K.; Sang, J. G.; Woo, G. C.; Zhang, B. Y. Evaluation of pedestrian winds around tall buildings by a numerical approach. *Meteorology and Atmospheric Physics* **2004**, *87*, 133–142.
7. Tunick, A. *A Two-Dimensional Meteorological Computer Model for the Forest Canopy*; ARL-MR-569; U.S. Army Research Laboratory: Adelphi, MD, 2003.
8. Chorin, S. E. A numerical method for solving incompressible viscous flow problem. *Journal of Computational Physics* **1967**, *2*, 12–26.
9. Jones, A. C.; Lauder, D. B. Lectures in mathematical models of turbulence; Academic Press: London, 1972, p 358.
10. Paterson, D. A;. Apelt, C. J. Simulation of wind flow around three-dimensional buildings. *Building and Environment* **1989**, *24*, 39–50.
11. Patankar, S. V. Numerical Heat Transfer and Fluid Flow, McGraw-Hill, New York 1980.
12. Johnson, G. T.; Arnfield, A. J.; Herbert, J. M. Coupling of an urban dispersion model and an energy budget model. *in Numerical Simulations in the Environmental and Earth Sciences*, Garcia, F. G.; Cisneros, G.; Fernandez-Eguiarte, A.; Alvarex, R., Eds.; Cambridge University Press: Cambridge, UK, 1997, pp 161–165.
13. Herbert, J. M.; Johnson, G. T.; Arnfield, A. J. Modelling the thermal climate in city canyons. *Environmental Modelling and Software* **1988**, *13*, 267–277.

14. Herbert, J. M.; Herbert, R. D. Simulation of the effects of canyon geometry on thermal climate in city canyons. *Mathematics and Computers in Simulation* **2002**, *59*, 243–253.

15. Kim, J.-J.; Baik, J.-J. A numerical study of the effects of ambient wind direction on flow and dispersion in urban street canyons using the RNG k – ε turbulence model. *Atmospheric Environment* **2004**, *38*, 3039–3048.

16. Baik, J.-J.; Kim, J.-J.; Fernando, H.J.S. A CFD Model for Simulating Urban Flow and Dispersion. *Journal of Applied Meteorology* **2003**, *42*, 1636–1648.

17. Yakhot, V.; Orszag, S. A.; Thangam, S.; Gatski, T. B.; Speziale, C. G. Development of turbulence models for shear flows by a double expansion technique. *Physics of Fluids A* **1992**, *4*, 1510–1520.

18. Kim, J.-J.; Baik, J.-J. A numerical study of thermal effects on flow and pollutant dispersion in urban street canyons. *Journal of Applied Meteorology* **1999**, *38*, 1249–1261.

19. Baik, J.-J.; Kim, J.-J. A numerical study of flow and pollutant dispersion characteristics in urban street canyons. *Journal of Applied Meteorology* **1999**, *38*, 1576–1589.

20. Versteeg, H. K.; Malalasekera, W. An Introduction to Computational Fluid Dynamics: The Finite Volume Method. Longman, Malaysia pp. 1995, 198–203 and 243–244.

21. Pullen, J.; Boris, J. P.; Young, T.; Patnaik, G. A comparison of contaminant plume statistics from a Gaussian puff and urban CFD model for two large cities. in press, Atmospheric Environment 2004, available online.

22. Boris, J. P. The threat of chemical and biological terrorism: preparing a response. *Computing in Science and Engineering* **2002**, *4*, 22–32.

23. Grinstein, F. F.; Fureby, C. From canonical to complex flows: Recent progress on monotonically integrated LES. *Computing in Science & Engineering* **2004**, *6*, 36–49.

24. Patnaik, G.; Boris, J. P.; Grinstein, F. F.; Iselin, J. P. Large scale urban simulation with the MILES approach. Annual AIAA CFD Conference, AIAA Paper 2003-4104, 2003, Orlando, FL.

25. Personal communication from R. Meyers, 27 January, 2005.

26. Calhoun, R.; Gouveia, F.; Shinn, J.; Chan, S.; Stevens, D.; Lee, R.; Leone, J. Flow around a complex building: comparisons between experiments and a Reynolds-Averaged Navier–Stokes approach. *Journal of Applied Meteorology* **2004**, *43*, 696–710.

27. Yamada, T. A numerical model study of turbulent airflow in and above a forest canopy. *Journal of the Meteorological Society of Japan* **1982**, *60*, 439–454.

28. Chan, S. T.; Ermak, D. L.; Morris, L. K. FEM3 model simulations of selected Thorney Island Phase I trials. *Journal of Hazardous Materials* **1987**, *16*, 267–292.

29. Ferziger, J. H.; Perić, M., Computational methods for fluid dynamics. 3rd Edition, Springer, Berlin, 2002, p 423.

30. Tunick, A. *Toward improving the efficiency and realism of coupled meteorological—acoustic computer models for the forest canopy*; ARL-MR-586; U.S. Army Research Laboratory: Adelphi, MD, 2004.

31. Munn, R. E. Descriptive micrometeorology. Academic Press, New York, 1966, p 245.

32. Press, W. H.; Teukolsky, S. A.; Vetterling, W. T.; Flannery, B. P. Numerical recipes in Fortran. 2nd Edition, Cambridge University Press, 1992, p 963.

33. Mahaffy, J.H. Solution of the finite volume equations. Internet document, www.personal.psu.edu/faculty/j/h/jhm/470/lectures/lec04.html (access 2005).

34. Tang, H. Mathematics of the finite element method. Internet document, math.nist.gov/mcsd/savg/tutorial/ansys/FEM/ (access 1995).

Distribution

ADMNSTR
DEFNS TECHL INFO CTR
ATTN DTIC-OCP (ELECTRONIC COPY)
8725 JOHN J KINGMAN RD STE 0944
FT BELVOIR VA 22060-6218

DARPA
ATTN IXO S WELBY
3701 N FAIRFAX DR
ARLINGTON VA 22203-1714

US MILITARY ACDMY
MATHEMATICAL SCI CTR OF EXCELLENCE
ATTN MADN-MATH LTC T RUGENSTEIN
THAYER HALL RM 226C
WEST POINT NY 10996-1786

SCI & TECHNLGY CORP
10 BASIL SAWYER DR
HAMPTON VA 23666-1293

US ARMY CRREL
ATTN CECRL-GP M MORAN
ATTN CERCL-SI E L ANDREAS
72 LYME RD
HANOVER NJ 03755-1290

US ARMY DUGWAY PROVING GROUND
DPG METEOROLOGY DIV
ATTN J BOWERS
WEST DESERT TEST CENTER
DUGWAY UT 84022-5000

NAV POSTGRADUATE SCHL
DEPT OF METEOROLOGY
ATTN P FREDERICKSON
1 UNIVERSITY CIR
MONTEREY CA 93943-5001

AIR FORCE
ATTN WEATHER TECHL LIB
151 PATTON AVE RM 120
ASHEVILLE NC 28801-5002

COLORADO STATE UNIV
DEPT OF ATMOS SCI
ATTN R A PIELKE
200 WEST LAKE STREET
FT COLLINS CO 80523-1371

DUKE UNIV PRATT SCHL OF ENGRG
DEPT OF CIVIL & ENVIRON ENGRG
ATTN R AVISSAR
HUDSON HALL-BOX 90287
DURHAM NC 27708

THE CITY COLLEGE OF NEW YORK
DEPT OF EARTH & ATMOS SCI
ATTN S D GEDZELMAN
J106 MARSHAK BLDG 137TH AND CONVENT AVE
NEW YORK CITY NY 10031

UNIV OF ALABAMA AT HUNTSVILLE
DEPT OF ATMOS SCI
ATTN R T MCNIDER
HUNTSVILLE AL 35899

NATL CTR FOR ATMOS RSRCH
ATTN NCAR LIBRARY SERIALS
PO BOX 3000
BOULDER CO 80307-3000

DIRECTOR
US ARMY RSRCH LAB
ATTN AMSRD-ARL-RO-D JCI CHANG
ATTN AMSRD-ARL-RO-EN W D BACH
PO BOX 12211
RESEARCH TRIANGLE PARK NC 27709

US ARMY RSRCH LAB
ATTN AMSRD-ARL-CI-C L TOKARCIK
ATTN AMSRD-ARL-CI-C
M VORONTSOV
ATTN AMSRD-ARL-CI-CN A TUNICK
(10 COPIES)
ATTN AMSRD-ARL-CI-CN G RACINE
ATTN AMSRD-ARL-CI-CS R MEYERS
ATTN AMSRD-ARL-CI-OK-T
TECHL PUB (2 COPIES)
ATTN AMSRD-ARL-CI-OK-TL
TECHL LIB (2 COPIES)
ATTN AMSRD-ARL-D J M MILLER
ATTN AMSRD-ARL-D J ROCCHIO
ATTN IMNE-ALC-IMS
MAIL & RECORDS MGMT
ADELPHI MD 20783-1197